Int J Thermophys (2009) 30:580–590
DOI 10.1007/s10765-008-0510-1

Texture and Porosity Effects on the Thermal Radiative Behavior of Alumina Ceramics

Olivier Rozenbaum · Domingos De Sousa Meneses · Patrick Echegut

Received: 23 July 2008 / Accepted: 10 September 2008 / Published online: 31 October 2008

Abstract Thermal and optical properties of ceramics are dependent on radiation scattering and cannot be determined by a knowledge of their chemical composition alone, as for single crystals. In this paper, extrinsic effects, such as roughness, porosity, and texture, on the spectral emissivity of alumina ceramics are investigated. Roughness effects have an influence mainly in the opaque zone; an important porosity dependence and the presence of a critical porosity threshold were observed in the semitransparent zone. Furthermore, it was shown that two ceramics with similar total porosities, but with different textures, possess radically different emissivities, showing that grain size, pore size, and spatial repartition of the grains are also crucial for an understanding of the thermal properties of the ceramics.

Keywords Ceramics · Emissivity spectra · High temperature · Infrared spectroscopy · Texture

This study was performed at CEMTHI laboratory.

O. Rozenbaum (✉)
Université d'Orléans, CNRS/INSU, Université de Tours,
Institut des Sciences de la Terre d'Orléans (ISTO), UMR 6113,
1A, rue de la Férollerie, 45071 Orléans Cedex 2, France
e-mail: rozenbaum@cnrs-orleans.fr

D. De Sousa Meneses · P. Echegut
Conditions Extrêmes et Matériaux: HauteTempérature et Irradiation (CEMTHI),
UPR 3079, 1D avenue de la Recherche Scientifique, 45071 Orléans Cedex 2, France
e-mail: desousa@cnrs-orleans.fr

P. Echegut
e-mail: echegut@cnrs-orleans.fr

1 Introduction

Precise characterization of the thermal radiation heat transfer efficiency of structural materials is mandatory to design and optimize devices sperating at high temperature such as glass-making furnaces or thermal shields. To determine these properties, direct measurement of the spectral emissivity is a must, as shown in the available literature on this subject (e.g., [1, 2]). The optical and radiative properties of single crystals and non-porous materials are relatively well known and completely defined by a knowledge of intrinsic parameters, such as the complex refractive index, and the thickness of the material alone [3–5]. Nevertheless, these properties are modified by extrinsic parameters in the case of porous materials such as ceramics. Some authors [6–12] have pointed out the effect of the structure of ceramics, the roughness, the porosity, the grain and pore size, the birefringence, and the role of impurities within the grain boundaries. However, as shown by Grimm et al. [8], Budworth [13], and Peelen [6], the effect of the birefringence is negligible compared to the pore size effect. Also, a knowledge of the chemical formula of a material alone is not sufficient to have a perfect understanding of the associated ceramic emissivity.

In this paper, it is shown how some extrinsic contributions impact the spectral emissivity of alumina ceramics. All the reported measurements were performed with a setup [2] that enables acquisition of accurate emissivity spectra of semitransparent porous and non-porous materials. After a brief description of the setup and the studied ceramics, influences of the porosity and the texture effect on the radiative properties of alumina ceramics will be reported and discussed.

2 Material and Method

2.1 Spectral Emissivity Measurement

The apparatus, previously described in detail [2], consists of a FTIR Bruker IFS 113v spectrometer which was enhanced with an external optical device that allows the measurement of infrared fluxes emitted by a sample and a blackbody furnace for identical geometrical conditions. To achieve very high temperatures (2,500 K) and to avoid parasitic flux due to hot closure confinement, CO_2 laser heating was chosen. The particular design of the heating configuration enables a quasi-homogeneous temperature over the measured sample area. The sample temperature was determined at a particular wavelength called the "Christiansen point" [1, 2]. Indeed, at this wavelength, polar dielectric materials such as oxide materials behave like a blackbody ($\varepsilon = 1$). This characteristic point suffers little change with temperature and was quasi-independent of the texture and material roughness. Hence, the temperature determination can then be obtained by using the spectrometer as a pyrometer at the Christiansen wavenumber. For alumina materials, the Christiansen wavelength is near 1,030 cm^{-1}.

For stability reasons and better precision, the temperature of the blackbody furnace was maintained at 1,673 K. So, the spectral emissivity of a sample at a temperature T was calculated by the following expression [14]:

$$\varepsilon(T) = \frac{\mathrm{FT}\left(I_{\mathrm{S}}^{\mathrm{mes}} - I_{\mathrm{RT}}^{\mathrm{mes}}\right)}{\mathrm{FT}\left(I_{\mathrm{BB}}^{\mathrm{mes}} - I_{\mathrm{RT}}^{\mathrm{mes}}\right)} \times \frac{P_{\mathrm{BB}} - P_{\mathrm{RT}}}{P_{\mathrm{S}} - P_{\mathrm{RT}}}$$

where FT is the Fourier transform, $I_{\mathrm{S}}^{\mathrm{mes}}$, $I_{\mathrm{BB}}^{\mathrm{mes}}$, and $I_{\mathrm{RT}}^{\mathrm{mes}}$ are the interferograms recorded, respectively, for the sample, the blackbody reference, and the room temperature parasite flux, and P_{S}, P_{BB}, and P_{RT} are the calculated Planck's functions at the sample temperature, the blackbody furnace, and a blackbody at room temperature, respectively.

2.2 Materials

The choice of several alumina ceramics with perfectly controlled characteristics was imposed by several constraints. The first was the necessity to obtain enough emitted energy in the mid-infrared range or, in other words, the necessity to select a material whose texture does not evolve with temperature, allowing high temperature measurements. Another was the fact that the samples must be good absorbers at the CO_2 laser frequency to be efficiently heated.

Two sets of high purity alumina ceramics covering a large range of porosity and with a fixed texture were obtained from an industrial supplier (Desmarquest) and from a French public laboratory (CEA-CEREM). Thereafter, the samples were labeled by the following nomenclature: Compound(Origin)-Porosity. So, a CEA's alumina ceramic with a porosity of X % will be named Al(C)-X. For the ceramics made by Desmarquest, the letter D was used for the classical process of fabrication and D′ for one particular ceramic. Indeed, most of the alumina ceramics fabricated by Desmarquest resulted from a classical industrial process from a biomedical powder (alumina α, purity 99.9 %). All these ceramics were made from powders with the same grain diameter (approximately 0.5 µm), and different porosities were obtained by using different sintering temperatures (Table 1). The only exception was the ceramic noted Al(D′)-23.2 that was made from a bimodal grain distribution, to study the effect of the texture. The second set of ceramics came from the CEA-CEREM laboratory and was made from an α alumina powder with a purity higher than 99.99 %. The powder was calcined at 1,273 K, to obtain larger grains, and then crushed. The resulting clusters were then sieved at 400 µm and pressed at 1,500 bar with an isostatic press to form alumina rods. Finally, different porosities were obtained by using different sintering temperatures (Table 1). As the only parameter that was varied during the fabrication process was the sintering temperature, the resulting ceramics possessed analogous texture and differed only by their porosity. Indeed, the observation of different ceramic fractures by scanning electron microscopy (SEM) was carried out to control the sintering effect and to obtain the average grain size and morphology (Figs. 1, 2, 3 and Table 1). For porosities (measured by geometrical measurements and helium pycnometry) between 3.8 % and 29.2 % (CEA samples), all the ceramics exhibited analogous morphology and spatial arrangement. The only significant change was the mean grain size that slightly increased along with the higher sintering temperatures. Furthermore, image analysis on Desmarquest ceramics (Al(D)-0.6 and Al(D)-3.5) showed that these materials have roughly similar grain size and spatial repartition. These sets

Table 1 Main properties of the studied ceramics

Origin	Sample	Total porosity (%)	Average grain diameter (μm)	Sintering temperature (K)
Desmarquest	Al(D)-0.6	0.6 ± 0.1	1–6	1,883
	Al(D)-3.5	3.5 ± 0.2	0.5–1	1,623
	Al(D′)-23.2	23.2 ± 0.4	5–50	2,003
CEA	Al(C)-3.8	3.8 ± 0.1	0.5–3	1,773
	Al(C)-4.1	4.1 ± 0.1	0.5–3	1,773
	Al(C)-4.3	4.3 ± 0.4	0.5–3	1,773
	Al(C)-9.1	9.1 ± 0.2	0.5–1.5	1,693
	Al(C)-9.6	9.6 ± 0.4	0.5–1.5	1,673
	Al(C)-10.3	10.3 ± 0.4	0.5–1.5	1,673
	Al(C)-20.6	20.6 ± 0.1	0.5–1	1,623
	Al(C)-28.6	28.6 ± 0.1	0.5–1	1,573
	Al(C)-29.2	29.2 ± 0.2	0.5–1	1,573

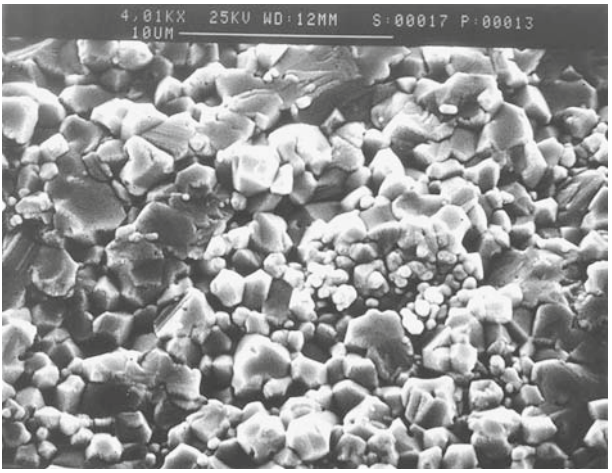

Fig. 1 Alumina ceramic Al(C)-3.8 (CEA). Sintering temperature: 1,773 K. Porosity: 3.8 %

of samples were then appropriate to study the influence of the porosity on the spectral emissivity.

In contrast, the bimodal grain distribution of the Al(D′)-23.2 sample belonged to the (5 to 50) μm range. Mercury intrusion porosimetry analysis showed that the mean pore size of this sample was 40 times higher than the mean pore size of the other ceramics (not shown here). The large pore size was explained by the presence of large grains (50 μm) that were responsible for the origination of the macropores.

Fig. 2 Alumina ceramic Al(C)-20.6 (CEA). Sintering temperature: 1,623 K. Porosity: 20.6 %

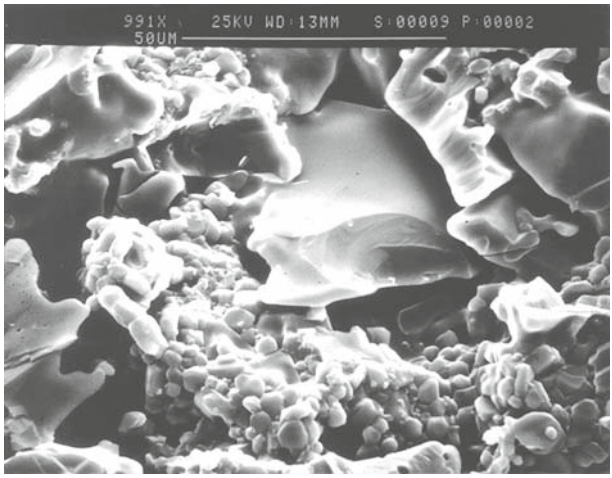

Fig. 3 Alumina ceramic Al(D′)-23.2 (Desmarquest). Sintering temperature: 2,003 K. Porosity: 23.2 %

3 Results

For a study of the porosity effect, all the emissivity spectra were acquired on one millimeter thick polished samples at 1,350 K to stay below the sintering temperature and retain the initial texture of the most porous ceramic. To ensure that the spectra obtained on a single sample were self-averaged, several measurements on different samples with identical texture and equivalent porosity (Table 1) were taken. For the sake of clarity, only sets of the more representative samples were retained in the following figures.

In the (400 to 1,300) cm^{-1} range (Fig. 4), alumina ceramics were opaque (phonon zone) and the optical properties were only due to the material surface. For longer wavelengths, i.e., between 1,300 cm^{-1} and 2,500 cm^{-1}, the absorption coefficient

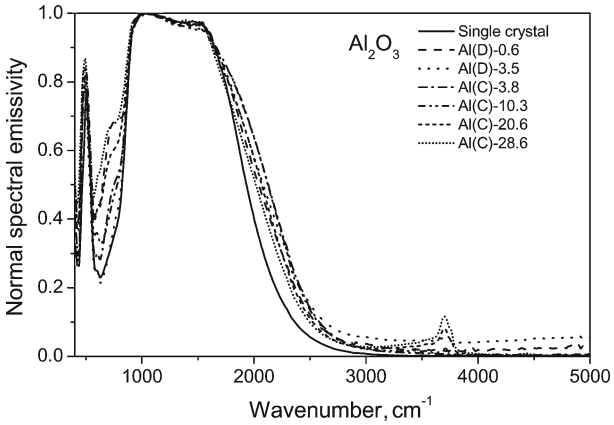

Fig. 4 Normal spectral emissivities of an alumina single crystal and alumina ceramics for various porosities (thickness = 1 mm, $T = 1,350$ K)

decreases and the material becomes semitransparent. For the most porous samples, broad bands appeared in the emissivity spectra between 2,600 cm^{-1} and 4,000 cm^{-1} (Fig. 4) and were not the only consequence of the porosity. The microscopic origin of these bands comes from the hydroxyl groups and trapped water molecules. These bands did not appear in dense ceramics because of their closed porosity and the fact, that, during their fabrication, they were sintered at higher temperatures by comparison with the most porous ones. Without these contributions, i.e., above 4,000 cm^{-1}, the absorption coefficient becomes intrinsically sufficiently weak to consider the material as transparent and the emissivity negligible [5].

The porosity effect was observed by the juxtaposition of the spectral emissivities of the CEA samples (Al(C)-3.8 to Al(C)-29.2) and the Desmarquest samples (Fig. 4). A rapid overview of this figure showed two different aspects of the porosity effect: a frequency shift of the transmissivity edge by comparing it to that of the single crystal, and an enhancement of the emissivity in the phonon wavenumber range (opaque zone).

3.1 Roughness Effect in the Opaque Zone

The porosity dependence on the spectral emissivity in the phonon range is shown in Fig. 5. With the porosity increase, a strengthening of the surface scattering was observed, which resulted in a progressive weakening of the reflection bands, and then an enhancement of the emissivity. Besides, in addition to these progressive modifications, the band shapes were markedly modified in comparison with those of the single crystal, but the band shapes did not evolve significantly with an increase in porosity between 500 cm^{-1} and 900 cm^{-1}. Several authors [10, 15–19] showed that the band shape of the spectral emissivity was dependent on the grain size and the grain shape constituting the surface of the sample. Several types of behaviors appeared according to the particle size and the value of the absorption coefficient K (e.g., [16]). For high values of the absorption coefficient (opaque zone), these authors showed that the

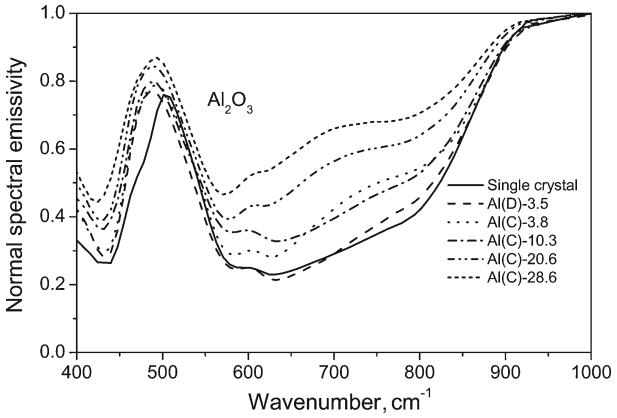

Fig. 5 Influence of the porosity in the phonon zone on normal spectral emissivities of alumina ceramics (thickness $= 1\,\text{mm}$, $T = 1,350\,\text{K}$). The normal spectral emissivity of an alumina single crystal (thickness $= 1\,\text{mm}$, $T = 1,350\,\text{K}$) was given as reference

particle size decrease induced a reflectivity drop leading to an increase of emissivity. Furthermore, Anderson and Ribbing [20] have pointed out that the spectral emissivity was also particle-shape dependent. Following their work, a distortion of the reflection band, near the longitudinal optic mode wavenumber ($850\,\text{cm}^{-1}$ for alumina), was due to surface defects with a spherical shape. This general trend was in accordance with the bump localized in the emissive spectra, around $720\,\text{cm}^{-1}$ (Fig. 5). Indeed, SEM images obtained on the ceramics of CEA showed that the grains were polyhedrons with quasi-spherical shape (Fig. 2).

3.2 Porosity Effect

The porosity dependence on the spectral emissivity in the semitransparent region is reported in Fig. 6, and the emissivity evolution with respect to the porosity is shown for three wavenumbers in Fig. 7. In this spectral range, ceramic emissivities were always higher than those of the single crystal. Furthermore, for small values of the total porosity ((0 to 5) % range) the emissivity increased as the ceramics became more and more porous. To our knowledge, few results related to this subject have been published [6–8, 11, 12, 21–23]. Some authors [19, 24] have determined by transmissivity measurements that, in the semitransparent region, radiation scattering inside ceramics was mainly due to the pores. Scattering by grain interfaces in a weak anisotropic material, such as dielectric oxides in the semitransparent zone, was always weak in comparison with the previous mode. With transmissivity measurements made on dense ceramics (<2 % of porosity), Grimm [8] showed that a density decrease, i.e., a porosity increase, strengthens radiation scattering (backscattering) and lowers the sample transmissivity (inducing an emissivity increase). These results are consistent with the present work and explain the observed phenomenon. Besides, for a higher total porosity, a change of behavior was observed since the emissivity decreased continuously (Fig. 7). This

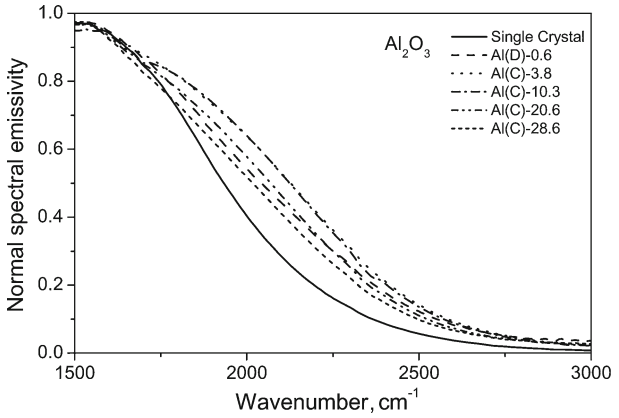

Fig. 6 Influence of the porosity in the transmission edge of alumina ceramics (thickness = 1 mm, $T = 1{,}350$ K, from CEA). The normal spectral emissivity of an alumina single crystal (thickness = 1 mm, $T = 1{,}350$ K) was given as reference

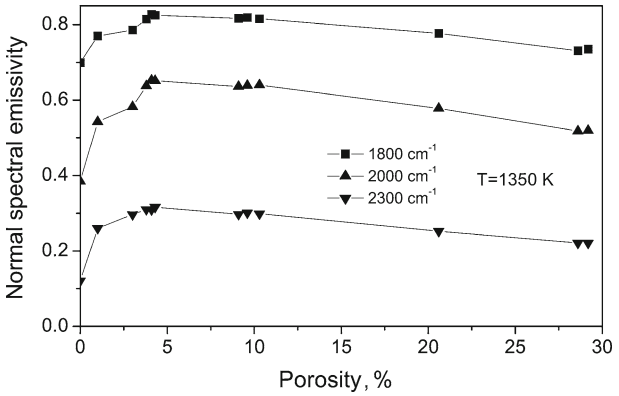

Fig. 7 Evolution of the normal spectral emissivity of alumina ceramics (thickness = 1 mm) versus porosity: $T = 1,350$ K

result shows the existence of a critical porosity for which the emissivity reaches its highest value in the semitransparent zone for this type of texture.

3.3 Texture Influence

As for porosity, the spatial repartition, grain size, and pore size, parameters that we call texture, influence mainly the radiative properties of a material. This point can be brought to the fore by a comparison between the Al(D′)-23.2 and Al(C)-20.6 samples that possess similar total porosities but very different textures as shown in Figs. 2 and 3. The main modifications between the spectral emissivity spectra of these two samples (Fig. 8) occur in the semitransparent zone. Unlike the other previously studied ceramics, the Al(D′)-23.2 ceramic has a much lower emissivity than the single crystal

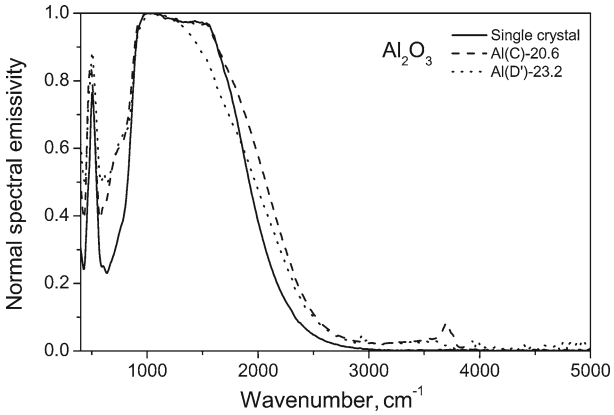

Fig. 8 Normal spectral emissivity of alumina ceramics (thickness $= 1\,\text{mm}$, $T = 1,350\,\text{K}$) with two different textures

between $1{,}300\,\text{cm}^{-1}$ and $1{,}800\,\text{cm}^{-1}$, and the spectral emissivity of this sample was radically different from the Al(C)-20.6 emissivity spectra. For longer wavelengths, the emissivity increases to become higher than those of the single crystal and tends to those of the Al(C)-20.6 sample in the transparent zone. A knowledge of only the total porosity is then not sufficient to predict the radiative behavior of porous materials and confirmed the importance of the texture information.

4 Discussion

What is the phenomenon that could explain the critical threshold shown in Fig. 7? For the lowest porosities, pores induce thermal radiation scattering that lengthens the mean travel of the radiation and then increases the apparent optical thickness of the media. Also, the radiation path inside the ceramic was longer in comparison with those performed in the single crystal of the same thickness. Hence, as the absorption is strengthened, the emissivity of the ceramic is greater than those of the single crystal. Furthermore, as the materials become more and more porous, scattering was more and more important, and the emissivity increases, up to a critical porosity threshold. However, above this threshold, scattering was so important that backscattering became more efficient and induced progressively a decrease of the apparent optical thickness of the ceramic. Then, the radiation was absorbed less and the emissivity was lowered.

This behavior for porosities lower than the critical threshold was encountered for samples where the backscattered part of the radiation was weak in comparison with the transmitted part or, in other words, for samples having a diffuse transmissivity higher than the diffuse reflectivity [5]. The opposite behavior was observed for a porosity higher than the critical threshold, i.e., for samples having a diffuse reflectivity higher than the diffuse transmissivity. The critical threshold represented the limit between a reflective (porosity $> 5\,\%$) and a transmissive behavior. All these explanations are in agreement with the results of a numerical simulation of radiation scattering in porous media [5]. For porosities higher than those presented in this paper, the optical thickness

of the ceramics can probably be less than the thickness of the single crystal and, as a result, the ceramic emissivity should be less than the emissivity of the single crystal.

These explanations enable an understanding of the behavior observed in Fig. 8 between two ceramics with the same total porosity but different textures. For wavenumbers higher than 1,800 cm^{-1}, these two ceramics possessed an emissivity higher than that of the single crystal. In this range, due to the weak absorption coefficient, the radiation mean path inside the sample was higher than the thickness of the single crystal. Also, the emissivities of the ceramics are higher than those of the single crystal as previously observed. For wavenumbers between 1,300 cm^{-1} and 1,800 cm^{-1}, the emissivity of the Al(D′)-23.2 ceramic was lower than that of the single crystal. A qualitative comparison of the texture of both ceramics shows that the mean pore size of the Al(D′)-23.2 ceramic is 40 times higher than the mean pore size of the Al(C)-20.6 ceramic (Figs. 2, 3). This difference was sufficient to change drastically the nature of the radiation scattering in the Al(D′)-23.2 ceramic. In this case, the mean size of the pore radius was about 10 µm, and radiation scattering roughly follows the laws of geometrical optics. Under this condition, backscattering is very efficient. Therefore, in a finitely thick sample such as this one (thickness $\sim$ mm), diffuse reflectance is much more important than diffuse transmittance. With these considerations in mind, it is concluded that the apparent optical thickness of the sample probed with radiation wavenumbers between 1,300 cm^{-1} and 1,800 cm^{-1} is less than that of the corresponding single crystal. In other words, only radiation originating in a small layer near the sample surface equal to the optical extinction length can contribute to the emissivity. On the contrary, for the CEA samples, the mean size of the pore radius was about 0.25 µm, a value too small for scattering to follow geometrical optics laws [5]. Furthermore, the ceramic grains are small enough to allow energy transport across the grain boundary interfaces leading to intergrain energy losses and resulting in frustrated, rather than total, internal reflection which, in turn, induces less efficient backscattering. For this sample and within this spectral range, the absorption coefficient followed the backscattering behavior and led to the observed result. Thus, the spectral radiative properties were completely dependent on the competition between the absorption coefficient (following the wavelength) and the radiative scattering.

5 Conclusion

In this paper, we showed the effect of extrinsic parameters such as porosity and texture on the thermal radiative properties of alumina ceramics. Even if the behaviors observed for these materials are not valid for all ceramics, this presentation pointed out the need to take into account these parameters. Besides, this paper emphasizes the different mistakes that could be made (and now avoided) in a laboratory, industry, or design department in which care is not exercised. As emissivity in the transparent zone depends on extrinsic parameters, it is not possible to predict the spectral value of emissivity from a knowledge of intrinsic parameters (refractive index and extinction coefficient) and the thickness of the material alone. Indeed, as explained above, the modifications in the semitransparent and transparent zones were essentially due to the

bulk texture and porosity. In the opaque zone, the increase and spectral modification of the emissivity were mainly due to the structure of the ceramic surface. These results show, for instance, the necessity to have the exact characteristics of a ceramic to measure correctly its temperature with an optical pyrometer. In the same way, these textural changes must be taken into account in the input data used for modeling the heat transfer inside processes at high temperature such as a glass-making furnace. In future work, it will be interesting to verify if the critical porosity threshold observed for alumina ceramics is highly texture dependent or not.

References

1. J.R. Markham, P.R. Solomon, P.E. Best, Rev. Sci. Instrum. **61**, 3700 (1990). doi:10.1063/1.1141538
2. O. Rozenbaum, D. De Sousa Meneses, S. Chermanne, Y. Auger, P. Echegut, Rev. Sci. Instrum. **70**, 4020 (1999). doi:10.1063/1.1150028
3. D. De Sousa Meneses, J.F. Brun, P. Echegut, P. Simon, Appl. Spectrosc. **58**, 969 (2004). doi:10.1366/0003702041655467
4. R. Siegel, J.R. Howell, *Thermal Radiation of Heat Transfer* (Taylor & Francis, Bristol, PA, 1992)
5. O. Rozenbaum, D. De Sousa Meneses, P. Echegut, P. Levitz, High Temp. High Press. **32**, 61 (2000). doi:10.1068/htwu257
6. J.G.J. Peelen, Sci. Ceram. **6**, 1 (1973)
7. J.G.J. Peelen, R. Metselaar, J. Appl. Phys. **45**, 216 (1974). doi:10.1063/1.1662961
8. E. Grimm, G.E. Scott, J.D. Sibold, Ceram. Bull. **50**, 962 (1971)
9. J.W. Salisbury, L.S. Walter, J. Geophys. Res. **94**, 9191 (1989). doi:10.1029/JB094iB07p09192
10. J.W. Salisbury, A. Wald, Icarus **96**, 121 (1992). doi:10.1016/0019-1035(92)90009-V
11. W.W. Chen, B. Dunn, J. Am. Ceram. Soc. **76**, 2086 (1993). doi:10.1111/j.1151-2916.1993.tb08337.x
12. R. Lopes, L.M. Moura, A. Delmas. High Temp. High Press. **31**, 213 (1999). doi:10.1068/htrt143
13. D.W. Budworth, Spec. Ceram. **5**, 185 (1970)
14. D. De Sousa Meneses, J.F. Brun, B. Rousseau, P. Echegut, J. Phys. Condens. Mat. **18**, 5669 (2006). doi:10.1088/0953-8984/18/24/008
15. R.J.P. Lyon, Econ. Geol. **60**, 717 (1968)
16. G.R. Hunt, R.K. Vincent, J. Geophys. Res. **73**, 6039 (1968). doi:10.1029/JB073i018p06039
17. J.E. Conel, J. Geophys. Res. **74**, 1614 (1969). doi:10.1029/JB074i006p01614
18. J.E. Moersch, P.R. Christensen, J. Geophys. Res. **100**, 7465 (1995). doi:10.1029/94JE03330
19. J.F. Mustard, J.E. Hays, Icarus **125**, 145 (1997). doi:10.1006/icar.1996.5583
20. S.K. Anderson, C.G. Ribbing, Phys. Rev. B **49**, 11336 (1994). doi:10.1103/PhysRevB.49.11336
21. D.W. Lee, W.D. Kingery, J. Am. Ceram. Soc. **43**, 594 (1960). doi:10.1111/j.1151-2916.1960.tb13623.x
22. T. Makino, T. Kunitomo, I. Sakai, H. Kinoshita, Heat Trans. Jap. Res. **13**, 33 (1985)
23. T. Burger, J. Kuhn, R. Caps, J. Fricke. Appl. Spectrosc. **51**, 309 (1997). doi:10.1366/0003702971940404
24. W.L. Dunn, J. Quant. Spectrosc. Radiat. Transf. **29**, 19 (1983). doi:10.1016/0022-4073(83)90141-3